Revista Mexicana de Física S **58** (2) 206–209 DICIEMBRE 2012

Phase Diagrams for Generalized Spin Ising Model by using Linear Chain Approximation and Monte Carlo Simulations

D. Peña Lara[a,*], H. Correa[b], and C.A. Lozano[c]
[a]*Departamento de Física, Universidad del Valle, A.A. 25 360, Santiago de Cali, Colombia.*
[b]*Laboratorio de Optoelectrónica, Universidad del Quindío, Armenia, Colombia.*
[c]*Grupo de Estadística y Matématica Aplicada, Pontificia Universidad Javeriana, Cali (Colombia).*

Recibido el 25 de junio de 2010; aceptado el 6 de octubre de 2010

The general Spin-σ Ising Model has been studied using Linear Chain Approximation (LCA) and Monte Carlo (MC) Simulations. Phase diagrams in reduced anisotropy as a function of reduced temperature plane were obtained, for special case of σ = 1 and 2, are qualitatively the same as those of the usual Mean Field Theory and Pair Approximation based on Bogoliubov inequality for the free energy. For the case σ = 1 and low temperatures there is a first- line and one second-order line, which are connected to special point so called tricritical point (TCP). For σ = 3/2, tricritical phenomena there is not, but there exists a first-order line separating phases m_1 = 3/2 and m_2 = 1/2 which ends at an isolated multiphase critical point. At the last, the phase diagrams for σ = 2 are similar to those for σ = 1, but the main difference is the existence of an additional ferromagnetic phase at low temperatures. For this case, the phase diagram shows reentrance transition lines behavior but could be an artifact of the present method. MC simulations were done on simple cubic lattices and in below cases are obtained general trend of the mean field like approach. Only for case σ = 3/2 the present results are very different with MF theory where the first-line transition does not terminate on the second-order transition line. In sum, it was shown that the phase diagram for the generalized Ising model does not depend on the method but is intrinsic to the model.

Keywords: Generalized spin Ising model; linear chain approximation; Monte Carlo simulations; phase diagrams.

Se estudió el modelo de Ising de espín general por la Aproximación de la Cadena Lineal (ACL) y las simulaciones de Monte Carlo (MC). Los diagramas de fases en el plano de la anisotropía reducida como función de la temperatura reducida que se obtuvieron, en particular para σ = 1 and 3/2 son cualitativamente los mismo reportados por la teoría de Campo Medio y de la Aproximación de Pares. Para σ = 1 y a temperaturas bajas, hay una línea de primer orden y otra de segundo, las cuales se conectadas en punto especial denominado punto tricrítico (PTC) y para σ = 3/2, no se presenta el PTC, pero hay una línea de primer orden que separa las fases m_1 = 3/2 y m_2 = 1/2 la cual finaliza en un punto crítico multifásico aislado. Para los casos σ = 1 y 2, los diagramas son parecidos con la diferencia que hay una fase ferromagnética adicional, a bajas temperaturas para σ = 2. Para este caso, los diagramas de fases muestran líneas de transición reentrante pero podría deberse a un artefacto del método utilizado. Las simulaciones MC se realizaron sobre redes cúbicas simples y en todos los casos se obtuvo resultados cuantitativamente comparables con la aproximación de campo medio (ACM). Sólo para el caso σ = 3/2, los resultados obtenidos difieren de ACM donde la línea de transición de primer orden no termina sobre la línea de segundo orden. En suma, se ha mostrado que el diagrama de fases para el modelo de Ising generalizado no depende del método sino que es intrínseco al modelo.

Descriptores: Modelo de Ising de espín generalizado; aproximación de la cadena lineal; simulaciones de Monte Carlo; diagramas de fases.

PACS: 68.35.Rh; 75.50.Ik; 75.10Hk

1. Introduction

The Hamiltonian for a general spin Ising model may be written in the form

$$H = -J\sum_{\langle ij\rangle}\sigma_i\sigma_j + \Delta\sum_i \sigma_i^2 \qquad (1)$$

where the first sum runs over all pairs of nearest neighbors in the N lattice sites, $J > 0$ is the coupling constant, Δ is the crystal field or parameter of anisotropy and the spins σ_i have values $-s$, $-s+1, \ldots, s-1, s$. When $\sigma = 1$, Hamiltonian (1) is so called Blume-Capel model [1,2] to describe critical-tricritical phenomena in magnetic systems. For general σ, this model been investigated through mean field approximation [3]. It has shown that for integer spins there exist one tricritical point and a disordered phase at low temperatures which are not present for semi-integer spins. In both cases, there are σ-dependent number $n\prime$ of first-order lines emerging from a multiphase point at T = 0 inside the ferromagnetic region. For integer spins, one has $n\prime$ = σ lines where $n\prime-1$ of them end up at independent isolated multicritical points while the other one joins the second-order transition line at the tricritical point. For semi-integer spins all the $n\prime$ =$\sigma - 1/2$ lines also terminate at independent isolated multicritical points.

2. The linear chain approximation

The thermodynamic properties of (1) can be calculated approximately by using the Bogolyubov variational principle [4]. According to this principle the best approximate free energy to the system described by H is the minimum of the left-hand side of the inequality

$$F_0 + \langle H - H_0\rangle_0 \geqslant F \qquad (2)$$

Where $F_0 = -k_B T\ln(\mathrm{Tr}\exp(-\beta H_0))$ is the free energy associated to a trial Hamiltonian H_0 = $H_0(\gamma)$, with γ standing for the variational parameter, $\langle H - H_0\rangle_0$ is the thermal average taken over the ensemble defined by H_0, and F is the exact free energy.

In the linear chain approximation (LCA) [5] we choose as a trial Hamiltonian H_0 of parallel linear chains, namely,

$$H_0 = \sum_{\substack{parallel\\chain}} \left(-J\sum_i \sigma_i\sigma_{i+1} + \Delta\sum_i \sigma_i^2 - \gamma\sum_i \sigma_i \right) \quad (3)$$

For $\sigma = 1$ and assuming periodic boundary conditions, the transfer matrix is

$$T = \begin{pmatrix} e^{K-D+g} & e^{-\frac{1}{2}(D-g)} & e^{-(K+D)} \\ e^{-\frac{1}{2}(D-g)} & 1 & e^{\frac{1}{2}(D+g)} \\ e^{-(K+D)} & e^{\frac{1}{2}(D+g)} & e^{K-D-g} \end{pmatrix} \quad (4)$$

with

$$K = \beta J, \quad D = \beta\Delta, \quad g = \beta\gamma. \quad (5)$$

A partial diagonalization of T is achieved through the matrix

$$U = \frac{1}{\sqrt{2}} \begin{pmatrix} 1 & 0 & 1 \\ 0 & \sqrt{2} & 0 \\ 1 & 0 & -1 \end{pmatrix}$$

leading to

$$V \equiv U^{-1}TU = \begin{pmatrix} V_{11} & V_{12} & V_{13} \\ V_{12} & V_{22} & V_{23} \\ V_{13} & V_{23} & V_{33} \end{pmatrix}$$

where

$$V_{11} = e^{-D}[e^{-K} + e^{K}\cosh(g)]$$
$$V_{12} = \sqrt{2}e^{-\frac{D}{2}}\cosh\left(\frac{g}{2}\right)$$
$$V_{13} = e^{K-D}\sinh(g)$$
$$V_{22} = 1$$
$$V_{23} = \sqrt{2}e^{-D/2}\sinh\left(\frac{g}{2}\right)$$
$$V_{33} = e^{-D}[e^{K}\cosh(g) - e^{-K}]$$

The eigenvalue equation is

$$\lambda^3 + a\lambda^2 + b\lambda + c = 0 \quad (6)$$

with

$$a = -[1 + 2e^{K-D}\cosh(g)]$$
$$b = 2e^{-2D}\sinh(2K) + 2^{-D}[e^{K} - 1]\cosh(g)$$
$$c = 2e^{-2D}[\sinh(K) + \sinh(2K)]$$

The solution of Eq. (6) are

$$\lambda_n = \frac{2}{3}\sqrt{p}\cos\left(\frac{1}{3}\cos^{-1}\left(\frac{q}{2\sqrt{p^3}}\right) + \frac{2n\pi}{3}\right) - \frac{a}{3} \quad (7)$$

with $n = 0, 1, 2$, and $p = a^2 - 3b$ and $q = 9ab - 2a^3 - 27c$.

To obtain the best approximate free energy per spin associated with H, we follow the minimization of Eq. (2) procedure mentioned above by setting $\delta F_0 + \lim_{N\to\infty}\langle H - H_0\rangle_0)/\delta g = 0$, where

$$F_0 = -\lim_{N\to\infty}\frac{k_BT}{N}\ln(\mathrm{Tr}T^N)$$
$$= -k_BT\ln\left(\frac{2}{3}\sqrt{p}\cos(\theta_n) - \frac{a}{3}\right) \quad (8)$$

here, θ_n denotes the value of $\cos^{-1}(q/2\sqrt{p^3})/3 + 2n\pi/3$ corresponding to the largest eigenvalue, λ_n. This leads to the result

$$g = (z-2)Km \quad (9)$$

with $m = -\delta F_0/\delta g$. It is not difficult to realize that the largest eigenvalue is

$$\lambda_n(K, D, g) = \lambda_0$$

Fort the case σ = 3/2 , the transfer matrix is

$$T = \begin{pmatrix} T_{11} & T_{12} & T_{13} & T_{14} \\ T_{12} & T_{22} & T_{23} & T_{24} \\ T_{13} & T_{32} & T_{33} & T_{34} \\ T_{14} & T_{24} & T_{34} & T_{44} \end{pmatrix} \quad (10)$$

where

$$T_{11} = e^{\frac{1}{4}(9K-9D+12g)} \qquad T_{12} = e^{\frac{1}{4}(3K-5D+4g)}$$
$$T_{13} = e^{-\frac{1}{4}(3K+5D-2g)} \qquad T_{14} = e^{-\frac{9}{4}(K+D)}$$
$$T_{22} = e^{\frac{1}{4}(K-D+2g)} \qquad T_{23} = e^{-\frac{1}{4}(D+g)}$$
$$T_{24} = e^{-\frac{1}{4}(3K+5D+2g)} \qquad T_{33} = e^{\frac{1}{4}(K-D-2g)}$$
$$T_{34} = e^{\frac{1}{4}(3K-5D-4g)} \qquad T_{44} = e^{\frac{1}{4}(9K-9D-12g)}$$

$$U = \frac{1}{\sqrt{2}} \begin{pmatrix} 0 & 1 & 1 & 0 \\ 1 & 0 & 0 & 1 \\ 1 & 0 & 0 & -1 \\ 0 & 1 & -1 & 0 \end{pmatrix}$$

and

$$U^{-1}TU \equiv V = \begin{pmatrix} V_{11} & V_{12} & V_{13} & V_{14} \\ V_{12} & V_{22} & V_{23} & V_{24} \\ V_{13} & V_{23} & V_{33} & V_{34} \\ V_{14} & V_{24} & V_{33} & V_{44} \end{pmatrix}$$

with

$$V_{11} = e^{\frac{1}{4}(K-D)}\cosh\left(\frac{g}{2}\right) + e^{-\frac{1}{4}(K+g)}$$
$$V_{12} = e^{-\frac{5D}{4}}\left[e^{-\frac{3K}{4}}\cosh\left(\frac{g}{2}\right) + e^{\frac{3K}{4}}\cosh(g)\right]$$
$$V_{13} = e^{-\frac{5D}{4}}\left[e^{-\frac{3K}{4}}\sinh\left(\frac{g}{2}\right) + e^{\frac{3K}{4}}\sinh(g)\right]$$
$$V_{14} = e^{\frac{1}{4}(K-D)}\sinh\left(\frac{g}{2}\right)$$
$$V_{22} = e^{-\frac{9D}{4}}[e^{\frac{9K}{4}}\cosh(3g) + e^{-\frac{9K}{4}}]$$
$$V_{23} = e^{\frac{9}{4}(K-D)}\sinh(3g)$$
$$V_{24} = e^{-\frac{5D}{4}}\left[e^{\frac{3K}{4}}\sinh(g) - e^{-\frac{3K}{4}}\sinh\left(\frac{g}{2}\right)\right]$$
$$V_{33} = e^{-\frac{9D}{4}}\left[e^{\frac{9K}{4}}\cosh(3g) - e^{-\frac{9K}{4}}\right]$$
$$V_{34} = e^{-\frac{5D}{4}}\left[e^{-\frac{3K}{4}}\cosh\left(\frac{g}{2}\right) + e^{\frac{3K}{4}}\cosh(g)\right]$$
$$V_{44} = e^{\frac{1}{4}(K-D)}\cosh\left(\frac{g}{2}\right) - e^{-\frac{1}{4}(K+g)}$$

3. Results and discussions

In Fig. 1 shows the LCA results for the global phase diagram in the reduced temperature $t = k_BT/zJ$ as a function of reduced crystal field ($d = \Delta/zJ$) plane for σ = 1, on a cubic simple lattice (z = 6) in comparison with traditional Mean Field Approximation (MFA) and Monte Carlo Simulations (MC). One can see that the results from LCA are systematically below the MFA results and roughly comparable to those from MC. First-order transition has been determined from the hysteresis curve of magnetization as function of reduced temperature for a constant d as is shown in Fig. 2a. The TCP was determined following the criterion used in [6] which consider the variation of the magnetization (order parameter m) as a function of d for a constant t, as depicted in Fig. 2b.

The global phase diagram for σ = 3/2 is shown in Fig. 3 where there is no TCP with the upper transition line being always second-order. The unique first-order transition line separating the two ordered phases (m_1 = 3/2 and m_2 = 1/2, m is the magnetization) terminates at an isolated multiphase crit-

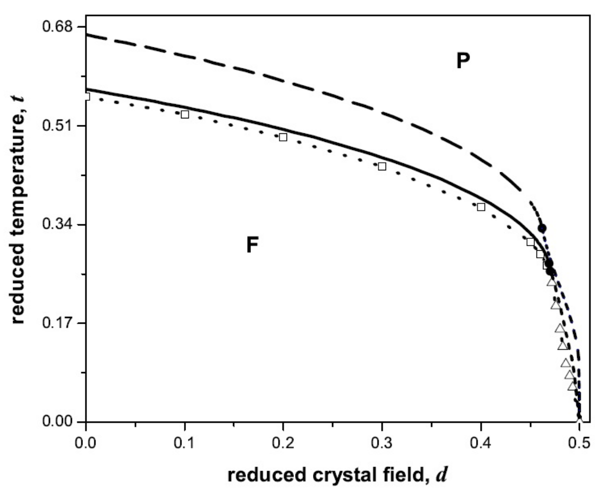

FIGURE 1. Phase diagram in the $(d - t)$-plane for the generalized Ising model with S = 1 obtained from: MFA (long-dashed line is second-order, dashed line is first-order); LCA (solid line is second-order, short-dashed line is first-order); MC (open squares are second-order, open triangular are first-order, dot lines are guide to the eyes). The full circles represent the corresponding TCPs.

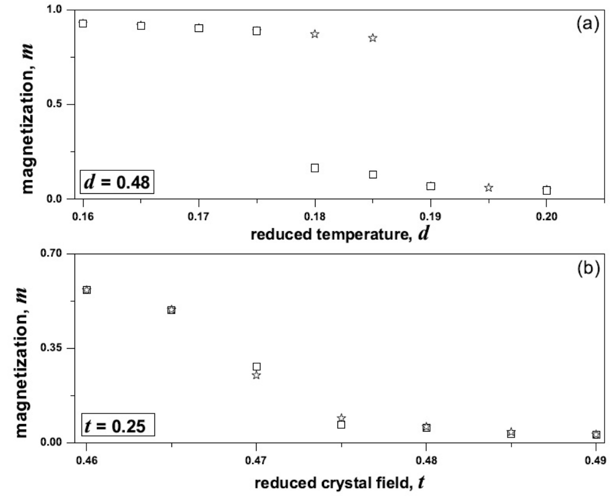

FIGURE 2. Some typical results from MC simulations. (a) Magnetization as a function of t for d = 0.48, open squares are for increasing t and open stars ones decreasing. The first-order transition temperature was estimated at t = 0.18(3) (b) Magnetization as a function of d for t = 0.26, open squares and stars have same means as (a). The tricritical temperature was estimated at t_T = 0.26.

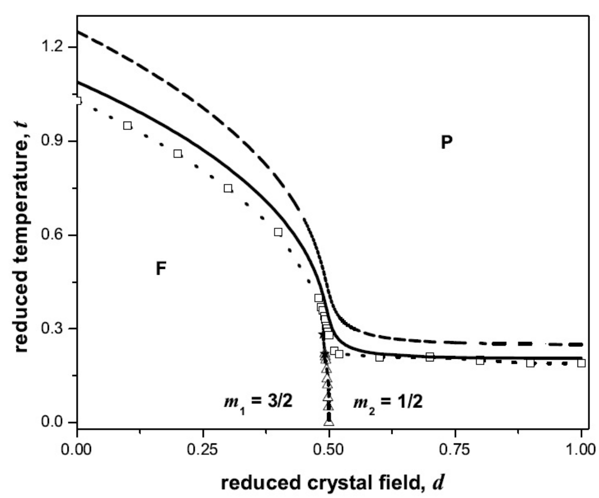

FIGURE 3. The same as Fig. 1 for σ = 3/2. In this case there is not TCP but there exist an isolated multiphase critical point denotes by $\star$.

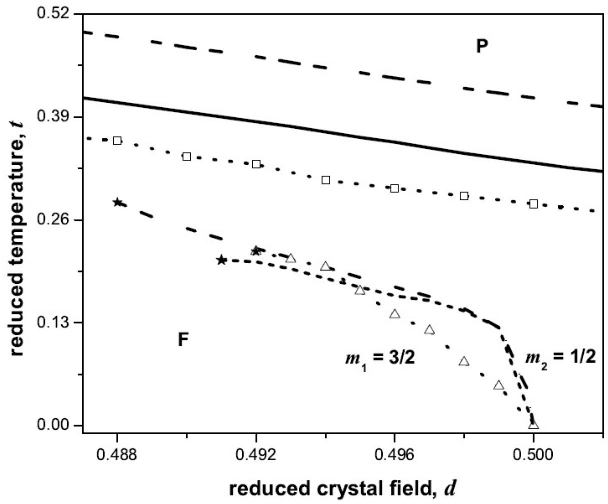

FIGURE 4. Low temperature phase diagram in the $d-t$-plane. The isolated multiphase critical point are represent by $\star$. There are two different ferromagnetic phases denote by m_1 = 3/2 and m_2 = 1/2 as $t \to 0$.

ical point, in complete agreement with traditional MFA [3]. Fig. 4 shows, with more details, the low temperature region of the phase diagram depicted in Fig. 3. The unique first-order transition line separating the two ordered phases terminates at an multiphase critical point far from the second-order transition in contrast with predicted by [7–9].

4. Conclusions

The general spin-S Ising model has been studied using the LCA and MC simulations. Full phase diagrams have been analyzed, specially in the low temperature region, where a number of first-order lines emerge. For σ = 1 the results from the LCA in three-dimensions are qualitatively the same with Monte Carlo simulations for a cubic lattice. So, the present results for S = 3/2 are contrary to the predictions from real space renormalization group approaches [7, 8], as well as previous Monte Carlo simulations [9]. They are, however, in qualitative agreement with those obtained from ordinary mean field calculations [3] and an exact formulation of the model on a Cayley tree [10]. Namely, the unique first-order transition line at low temperatures does not terminate on the second-order transition line.

∗. Corresponding author: Tel.: +57-2-3394610; fax +57-2-339 3237 e-mail: diego.pena@correounivalle.edu.co

1. M. Blume, *Phys. Rev.* **141** (1966) 517.
2. H.W. Capel, *Physica* **32** (1966) 966.
3. J.A. Plascak, J.G. Moreira, and F.C. Sá Barreto, *Phys. Lett. A* **173** (1993) 360.
4. H. Falk, *Amer. J. Phys.* **38** (1970) 858.
5. H.A. Kramers and G.H. Wannier, *Phys. Rev.* **60** (1941) 252.
6. A.K. Jan and D.P. Landau, *Phys. Rev. B* **22** (1980) 445.
7. S. Moss de Oliveira, P.M.C. de Oliveira, and F.C. Sá Barreto, *J. Stat. Phys.* **78** (1995) 1619.
8. A. Bakchich, A. Bassir, and A. Benyoussef, *Physica A* **195** (1993) 188.
9. F.C. Sá Barreto and O.F. de Alcantara Bonfim, *Physica A* **172** (1991) 378.
10. M.N. Tamashiro and S.R.A. Salinas, *Physica A* **211** (1994) 124.